EFFECT OF ACETIC ACID, pH AND MEG ON THE CO$_2$ TOP OF THE LINE CORROSION

C. Méndez, M. Singer, A. Camacho, S. Hernández, S. Nesic
Ohio University - Institute for Corrosion and Multiphase Technology

Y. Gunaltun,
Total Exploration Production
92069 Paris La Defense - France

M. Joosten
ConocoPhillips
Barlesville, OK 74004 - USA

Y. Sun
BP
Houston, TX 77079-2696 - USA

P. Gabbetta
ENI
Milano, 20097 San Donato Milanese - Italy

ABSTRACT

This research work presents a study of Top of the Line Corrosion (TLC) on carbon steels in the presence of carbon dioxide and acetic acid. The influence of different parameters such as the presence of mono-ethylene glycol (MEG) and the use of pH control were studied in a 4" diameter flow loop. Two sets of experiments were conducted; one at 70ºC, high CO$_2$ partial pressure and a "critical" condensation rate and another one at 80ºC, low CO$_2$ partial pressure and a high condensation rate. Weight loss techniques and surface analysis were used to evaluate the corrosion rate and products. It was found that the presence of HAc at the concentrations evaluated does not affect the general corrosion rate at the top of the line. Top of the line corrosion rates correlate with the De Waard / Lotz estimate of 10% of bottom of the line rates[15]. It is believed that the corrosion mechanism is still controlled by CO$_2$ partial pressure at the experimental conditions evaluated in this study. The presence of MEG has not shown any effect on TLC due to the fact that the condensation rate was kept constant. The use of pH control in the supply

is believed to limit the amount of HAc in the condensed water. No clear evidence of localized corrosion or pits can be reported at this stage of the study due to the short time of exposure.

Keywords: Top of the Line Corrosion, carbon dioxide, acetic acid, pH control, MEG, condensation rate.

INTRODUCTION

TLC occurs when, in multiphase stratified flow or during wet gas transportation, water vapor condenses on the internal walls of the pipeline due to the heat exchange occurring between the pipeline and its surroundings (e.g., offshore or arctic production). Water vapor condenses on the colder walls, forming a thin film of liquid which is enriched in aggressive species, such as organic acids and carbonic acid which comes from the dissolution of carbon dioxide (see Figure 1).

Gunaltun[1] reported that the corroded pipe wall can be divided into three parts:
- The bottom of the pipe, where the corrosion is uniform and where the corrosion rate can be lowered with the use of inhibitors.
- The sidewall of the pipe, where the condensed water drains to the bottom. The corrosion is also uniform, but inhibitors are not efficient.
- The top of the line, where a protective iron carbonate layer can be formed in certain cases, inhibitors are not effective, and localized corrosion occurs.

The main parameters influencing the TLC, as described in many papers[2-7], are the bulk temperature, partial pressure of carbon dioxide, gas velocity, and condensation rate. All of these parameters influence the corrosion rate in a complex way, but a common behavior has been reported:

- At low condensation rates, a protective film of iron carbonate appears at the surface of the pipe exposed to TLC, which lowers the corrosion rate. The formation of this film is explained by the iron saturation of the liquid film and the precipitation of corrosion product.

- At high condensation rates, saturation cannot be reached, and the corrosion rate can be on the order of several mm/y. The corrosion rate is governed by the rate of the corrosive reaction and the rate of condensation. The former increases the amount of iron in the liquid film, while the latter decreases it. The corrosion rate depends on the balance of these two counteracting effects.

The corrosion rate is governed by the rate of the corrosive reaction and the rate of condensation. The former increases the amount of iron in the liquid film, while the latter decreases it. The corrosion rate depends on the balance of these two counteracting effects.

In 2002, Vitse[8] completed a study on TLC in presence of carbon dioxide in the same experimental loop used in this work. He presented several new observations regarding the influence of some parameters on the TLC:

- As the carbon dioxide dissolves in the condensed water at the top of the line, it becomes responsible for the corrosivity of the liquid film. Consequently, it is believed that an increase in the CO_2 partial pressure can only increase the corrosion rate. However, the partial pressure of CO_2 shows little influence on the corrosion rate at low temperature (<50ºC) and high condensation rate or at high temperature (>90ºC) and low condensation rate. On the other hand, at high temperature and high condensation rate, the influence is more significant. This can be explained by the fact that at a low condensation rate, it is easier to saturate the condensed liquid film with corrosion products (iron ions

coming from the metal dissolution), increasing the pH and retarding the kinetics of the CO_2 corrosion reaction. At a high condensation rate, saturation of the condensed liquid film may not be possible, and the pH is more sensitive to the influence of the partial pressure of CO_2.

- The gas velocity is found to have a direct effect on the condensation rate that in turn can affect the corrosion rate. High gas velocity enhances the mass and heat transfer in the gas phase which results in an increase in the condensation rate.

- The condensation rate has a complex influence on the corrosion rate and is influenced by all other parameters. The corrosion rate increases significantly when the condensation rate reaches a certain threshold. This observation stems for the theory that the saturation level of corrosion products in the condensed film controls the corrosion rate. If the condensation rate is high enough that it prevents the liquid film from reaching saturation, the corrosion rate will depend on the corrosivity of the liquid phase. If the condensation rate is low, super-saturation can be reached, and this leads to the formation of an iron carbonate scale, which is protective at high temperatures only.

The effect of organic acids (acetic acid, in this work) on CO_2 corrosion has been investigated by several authors[9-11, 20]. In CO_2 corrosion, it is known that the presence of acetic acid in the liquid phase leads to an increase in the general corrosion rate. It is believed that acetic acid influences the corrosion process in two ways which are practically undistinguishable. First, the acetic acid dissociates to form acetate and hydrogen ions. It acts as a proton provider (it will decrease the pH of the solution and act as a buffer that prevents pH increases due to corrosion products). Secondly, the remaining acetic acid that did not dissociate (called free acetic acid) is believed to be reduced directly on the metal surface (in a similar way as carbonic acid). The contribution on the proton reduction and the direct reduction of acetic acid at the metal surface increase the overall cathodic current and enhance the anodic reaction (metal dissolution). In a CO_2 environment, the degree of this influence depends on the free acetic acid/carbonic acid ratio. It is also proposed that the presence of acetate could have an effect on the properties of the carbonate layer and change its potential protectiveness. Regarding TLC, the same observation can be made[12]. Acetic acid is volatile, so it can be transported in the gas phase and condenses with the water on the walls of the pipe.

Monoethylene glycol (MEG) is often used in the transportation of wet gas in order to prevent the formation of hydrates which can plug the pipelines. It is also known that glycol has a strong effect on CO_2 corrosion[13] mainly because it affects the solubility of CO_2 in the liquid phase. Data taken from Oyevaar, et al.,[14] show that the solubility of CO_2 in a water/glycol mixture first decreases as the mass percentage of glycol increases until a threshold value of 60% is reached, after which the solubility increases strongly. Regarding TLC, it is important to notice that the presence of glycol reduces the partial pressure of water by absorbing it from the gas phase[15]. The drying action of injected glycol will lower the dewpoint of the gas. For this reason, it is expected to have a reduction on the condensation rate in the presence of water/glycol mixtures.

The control of pH is a common corrosion mitigation method and has been used with success in gas condensate pipelines[16, 17]. It consists of the increase of pH in the water phase by injecting sodium bicarbonate or sodium hydroxide. It facilitates the formation of a dense iron carbonate product on the metal surface which has good protective properties against corrosion. Film properties such as thickness, porosity, and adherence therefore become very important. At high pH, the amount of undissociated HAc in the water phase is significantly reduced thus discouraging its evaporation and subsequent condensation at the top of the line. However, the success of this technique has been proven at the bottom of the line where the liquid is flowing, but not yet at the top of the line.

EXPERIMENTAL PROCEDURES

Experimental loop

The Institute for Corrosion and Multiphase Technology at Ohio University has built an experimental flow loop especially designed for the study of the Top of the Line Corrosion.

Figure **3** is a schematic representation of the loop. The flow loop, mainly made of stainless steel 316, can be divided in three main parts: the tank, the pump and the loop.

- The tank is used for the liquid phase conditioning and heating. It is filled with de-ionized water or a typical gas-condensate produced water (called later on "brine"). MEG, sodium bicarbonate and acetic acid are then added to reach the requirements of the tests. Two immersion heaters control the temperature. The mixing of water vapor and the gas phase (carbon dioxide and nitrogen) occurs at the upper part of the tank.
- The pump moving the gas is a positive displacement progressive cavity pump. It is continuously lubricated with liquid from the tank.
- The 4" diameter flow loop is 30 meters long and horizontally leveled. The gas mixture of water vapor and carbon dioxide (or a mixture of carbon dioxide and nitrogen) flows along the pipe and the condensation of water occurs due to the gradient of temperature across the pipe wall in the cooled section of the loop. The test section where the measurements are taken is located 8 meters downstream the exit of the tank. The test section (see Figure 4) is a 1.5 meters long pipe spool. It has four probe ports (two at the top, two at the bottom). The copper coils surrounding the pipe act as a heat exchanger. Samples of condensed liquid and in-situ pH measurements can be taken at the test section.

The experimental procedure is as follow: the tank is first filled with 1 m^3 of liquid (de-ionized water or produced water (brine) with or without MEG) and carbon dioxide (and nitrogen in some cases) is injected in the loop at a specific pressure. The liquid phase is then heated up to the specific temperature by two electrical resistance heaters. The pump is started and the vapor-gas mixture flows around the loop. The de-oxygenation is done by de-pressurizing several times until the concentration of oxygen is low (<50 ppb). Oxygen concentration is measured using colorimetric test kits. The condensation rate in the test section is carefully adjusted using a system of cooling coils surrounding the test section. The amount of liquid that condenses inside the line is collected at the end of the test section. When the condensation rate stabilizes, the corrosion probes are introduced in the test section and the experiments begin. A data acquisition device is used in order to continuously measure the inlet and outlet temperature of the gas and of the cooling liquid at the test section, the total pressure, the condensation rate and the cooling liquid flow rate.

Liquid phase specification

In experimental SET 1, a brine that simulates the produced water from a gas-condensate field is used as the liquid phase. The composition of this brine is presented in Table 1.

In experimental SET 2, de-ionized water is used as the liquid phase.

Acetic acid concentration

The acetic acid (HAc) concentration is adjusted by adding a calculated amount of pure HAc in the tank. The acetic acid is first de-oxygenated before being introduced into the tank using a high-pressure vessel connected to the tank. The concentration distribution of free HAc and acetate (Ac^-) in the tank is calculated from the measured value of pH. The total acetic acid concentrations in the tank and in the condensed water are then verified using an ion chromatograph.

Iron and oxygen concentration measurements

Liquid samples are taken regularly from the liquid phase in the tank and from the condensed water at the test section. The oxygen concentration is required to be lower than 50 ppb in each test. The iron concentration is measured at the tank and at the test section for each test.

Glycol concentration

The MEG used for the tests is a technical grade glycol. The quality of the glycol was evaluated in a glass cell by using the linear polarization technique as described by Gulbrandsen[13]. Results obtained with a mixture 50% MEG were in agreement with a corrosion rate reduction factor of 30% reported by Gulbrandsen[13]. All experiments were done with MEG coming from the same batch of production to avoid difference in composition that could affect the results.

pH measurement and pH control

The pH of the liquid phase of the tank as well as of the condensed water at the test section are measured for each test. It is known that pH measurements with high MEG concentration using a pH-meter calibrated in aqueous pH standards are in error due to the large change in solvent properties[13]. For practical reasons, aqueous pH buffer are used to calibrate the pH meter and no correction in the reading are made in this report. The values of pH reported are expected to be slightly more acidic than in reality.

In experiments with pH control, the desired value is achieved by adding sodium bicarbonate in the liquid phase of the tank. The pH is measured at system pressure in exit streams from the bottom of the tank and the bottom of the test section.

Condensation rate measurement

A system of coils installed around the test section is used as a heat exchanger. A specific flow of water is sent through the coils in order to cool down the walls of the pipe and to simulate condensation condition. A device located downstream of the test section (see Figure 4) allows the measurement of the condensation rate. The liquid that condenses on the inner walls of the pipe is collected in this device over time and the rate of condensation is then calculated in $ml/m^2/s$ (the calculation assumes that condensation occurs uniformly on the entire inner pipe surface). Two levels of condensation tested are presented in this paper: critical condensation rate and high condensation rate. The critical condensation rate represents the level of condensation at which the TLC rate cannot be neglected[18]. The high condensation rate exceeds the critical condensation rate and is representative of field conditions.

Corrosion rate measurement

The corrosion rate measurement starts once the system is at equilibrium. The corrosion rates are measured with weight loss coupons made of AISI 1020 and API X65 carbon steel. Samples consisting of cylindrical coupons (0.76 cm internal diameter, 3.17 cm external diameter, and 0.5 cm thickness) with an exposed area of 7.44 cm^2 are polished using isopropanol as coolant on silicon carbide papers up to 600 grit. After this preparation, they are covered with liquid Teflon on the edges and bottom. After 4 to 6 hours of curing at ambient conditions, the samples are held at 200°C in an oven for four hours. The uncovered steel surface is then re-polished with 600 grit silicon carbide paper wetted with isopropanol, cleaned, dried, and weighed. A picture of a coupon after preparation is shown in Figure 2. The coupons are then flush mounted on the internal pipe wall of the loop by using a specially designed probe holder. Therefore, only one face of the coupon is in direct contact with the corrosive environment. Two coupons are placed in the top position and two in the bottom. The exposure time is between 48 and 72 hours in all experiments. Upon removal from the loop, the coupons surface is flushed with isopropyl alcohol, to dry it and photographs of the surface are taken. The weight of the coupon after test is registered, and the ASTM G1 standard is followed to remove the corrosion products and determine the corrosion rate by weight loss. One coupon is generally used for weight loss, and the other is preserved for corrosion product evaluation on the top and bottom by scanning electron microscopy (SEM) or energy dispersion analysis (EDS). Some experiments are repeated. SEM analysis is done on the TOP samples with and without corrosion products and cross section analysis are done on most of the top samples and some of the bottom samples.

On two experiments, corrosion rates are also measured using an Electrical Resistance probe (ER probe). The sensing element is first polished and cleaned with isopropanol. As soon as the system reaches equilibrium, the ER probe is inserted, flush-mounted to the internal wall of the pipe and connected to the data acquisition to monitor the temperature of the sensing element and determine the metal loss with time. When the probe is pulled out of the pipe, the surface is flushed with alcohol and cleaned.

Materials Characterization

Two types of steel are tested: AISI 1020, purchased as a solid bar and API X-65 carbon steel from a piece of field pipe line (33 cm outside diameter pipe section, 3.8 inch thickness). These steels will be designated 1020 and X65 respectively. The chemical analyses of both materials are shown in Table 2. The fourth and fifth columns on this table shows the requirements specified on the standards for both materials.

Figure 5 shows the microstructure of longitudinal and transversal cuts of the X65 carbon steel. Figure 6 shows the microstructure of the 1020 carbon steel. In this case, only the face of the coupon that would be in contact with the fluid is evaluated. Cuts are made using cooling fluids and the proper saws to avoid modifications of the microstructure.

The microstructure of the X65 is finer in the longitudinal direction, probably as a result of processing. Figure 5 shows a microstructure typical of a micro-alloyed thermo-mechanical controlled processing (TMCP) pipeline steel. Iron carbide could be distributed in spheroidized form instead of a lamellar arrangement. Hardness measurements are recorded in Table 3.

The 1020 microstructure shows a typical ferritic (carbon in alpha iron)/pearlitic (lamellar microstructure of alternate α-iron and iron carbide Fe_3C) matrix, which is expected for this

hypoeutectoid steel (carbon content less than 0.8%). There is a homogeneous distribution of ferrite and pearlite.

Table **3** shows the hardness results obtained from the two materials tested, and the values shown are the average of ten readings. Also, by converting these values[18], approximate tensile strengths were calculated and compared with the values designated for those metals in the standards. The 1020 carbon steel showed a hardness of 84.3 HRB, and the calculated tensile strength is above the minimum requirements of the standard. The X65 showed a difference in hardness with direction. This change in hardness is consistent with the change in microstructure described previously.

Test matrix

Table 4 and Table 5 show the detailed conditions for each experiment. The tables present the experimental matrices (CO_2 partial pressure, gas temperature, condensation rate, glycol concentration, pH control, acetic acid concentration in the liquid phase of the tank) as well as a complete set of measurements done throughout the tests (pH measurement, iron and acetic acid concentrations at the tank and at the test section (condensed water)).

The experiments reported in this paper can be divided in two groups which show similar characteristics: SET 1 and SET 2.

The eight experiments related to SET 1 are obtained at 80°C with low CO_2 partial pressure and a superficial gas velocity of about 5 m/s. The liquid phase is based on the brine presented in Table 1. Each experiment is done only one time.

The four experiments related to SET 2 are obtained at 70°C with a high CO_2 partial pressure, and a velocity of about 3m/s. The liquid phase is made of de-ionized water. The condensation rate is fixed at the critical level and does not vary. Each experiment of SET 2 is done in duplicate.

Some of the major parameters that affect TLC are investigated in both sets of experiments:

- **Acetic acid**. The effect of acetic acid (up to 4000 ppm of overall acetate species in the liquid phase) is investigated. A differentiation is made between the free acetic acid concentration (free HAc) which represents the undissociated acetic acid concentration and the total acetic acid concentration which includes all acetate containing species (Free HAc and Ac-). The acetic acid concentration (measured and calculated) for all experiments is presented in Table 4 and Table 5.

- **Condensation rate (SET 1)**. Two condensation rates are investigated: critical and high. The critical condensation rate corresponds to a cooled pipeline condition where problems of TLC are expected to appear. A high condensation rate represents a higher level of cooling compared to the critical one.

- **pH control**. A feasibility study for the pH stabilization technique is done. The pH varies from the "pure" pH in condensed water (approximately 4), up to pH 7 to evaluate its effect on reduction of the corrosion rate;

- **Glycol**. The effect of glycol is investigated (0 or 50% in weight of the liquid phase of the tank);

<div align="center">

RESULTS

</div>

CORROSION RATE MEASUREMENTS

Due to the confidentiality of the results, only the trends (normalized corrosion values) will be reported here. The values are calculated by dividing the actual corrosion rate with the maximum corrosion rate of the entire series of tests. The normalized results qualitatively reveal the trends in the data and the influence of the key parameters.

General corrosion rate measurements are presented in Figure 7 (for SET 1) and Figure 8 (for SET 2).

Some remarks related to the plots shown in the figures:

- The weight loss corrosion rate values shown are time-averaged value (over the entire duration of the experiment) as well as space-averaged (over the entire area of the coupon).
- The numbers shown above the bars on the plots correspond to the number of times the experiment was repeated for a given set of conditions.
- Error bars denote the maximum and the minimum values obtained.
- Two values can be extracted from the measurements taken with ER probes: an average corrosion rate over the entire duration of the experiment, and a stable corrosion rate which is the stabilized value obtained at the end of the experiment.

Influence of the CO_2 partial pressure

The influence of the CO_2 partial pressure is studied in experiments 1-0 of SET 1 and 2-0 of SET 2 where the CO_2 partial pressure is increased from a low to a high level. It is important to notice that in SET 1 a brine is used as the liquid phase while it is de-ionized water for SET 2. It is so far difficult to expect any major impact of the mineral composition of the liquid phase on the general top of the line corrosion rate. Therefore, the results obtained in SET 1 and 2 are directly compared.

Top of the line

The corrosion rate obtained at a low CO_2 partial pressure is 25% lower than at a high partial pressure. In these experiments CO_2, when dissolved into the liquid phase, is the main corrosive component. Therefore, the higher the CO_2 partial pressure is, the higher the concentration of carbonic acid as well as protons is in the condensed water leading to a more corrosive environment.

Bottom of the line

The same observations can be made at the bottom of the line where the corrosion rate is more than two times higher for a high CO_2 partial pressure compared to a low CO_2 partial pressure.

Influence of the condensation rate

The influence of the condensation rate is studied in experiments 1-0 and 1-1 of SET 1 where the condensation increases from the critical to the high level.

Top of the line

An increase in the condensation rate from critical to high level does not show any influence on the corrosion rate which remains constant. However, the general corrosion rate is expected to increase with the condensation rate only if one is below the critical (threshold) value and the other one is higher. It is also important to mention that this experiment was not repeated and that only one weight loss result is available. The margin of error could explain why the results are so similar.

Bottom of the line

It is difficult to explain any influence of the condensation rate at the bottom of the line. Due to gravity forces, liquid accumulates at the bottom which is constantly in contact with a significant amount of liquid whatever the condensation rate is. However, the results show that the general corrosion rate decreases by one third when the condensation rate increases. This is most likely a random variation in the data set.

Influence of the glycol concentration

The influence of the glycol is studied in experiments 1-1 and 1-2 of SET 1and in experiments 2-0 and 2-1 of SET 2 where glycol is introduced in the liquid phase of the tank in order to reach 50% in weight.

Top of the line

In SET 1, the introduction of glycol decreases the general corrosion rate when in SET 2 the corrosion rate remains the same. It should be mentioned that glycol is used to prevent hydrate formation, which is mainly a flow assurance problem and not a corrosion problem. The presence of glycol reduces the water vapor pressure. Therefore, at the same temperature, the water content in the saturated gas will be lower. For this reason, the expected impact of glycol on TLC is to decrease the rate of condensation and consequently the rate of corrosion. However, in these experiments the condensation rate is set at a specific value (High for SET 1 and Critical for SET 2) by adjusting the water flow on the cooling device surrounding the test section. At these conditions, the amount of condensed liquid and the dynamic of the condensation process are expected to be the same in the presence and in the absence of glycol. Since almost no glycol is present in the condensed liquid (glycol evaporates poorly at these temperatures), the only influence that glycol could have on the TLC has been masked. In order to evaluate the more realistic impact of the glycol on TLC, it has been decided for future experiments to set a specific condensation rate without glycol (by setting a specific cooling rate at the test section) and then to introduce the glycol without a further adjustment of the cooling conditions. The addition of glycol will change the condensation rate, which corresponds better to the case in the field. This way a lower condensation rate is expected which may lead to a lower corrosion rate.

Bottom of the line

The addition of glycol lowered the corrosion rate of approximately 40% for SET 1 and 98 % for SET 2. According to Gulbransen[13], a 33% reduction in the corrosion rate of X65 would be expected in the presence of 50% glycol at 1 bar of CO_2 and room temperature. In the test section, the condensed liquid contained approximately 5% glycol (measured value). Therefore, a significant reduction in the corrosion rate observed was not expected. Regarding the experiment of SET 2, where the corrosion rate

is reduced of 98%, no layer is visible on the surface of the coupon, which has bright colors, and the bare metal can be seen in some areas. The reasons for such a behavior are still under investigation.

Influence of the HAc concentration

The influence of the HAc concentration is studied in experiments 1-2 and 1-3 of SET 1and in experiments 2-1 and 2-2 of SET 2. It is important to mention here that the parameter that is taken into account is the free acetic acid concentration, not the total acetic acid concentration. The acetic acid dissociates in solution (depending on the pH) to form acetate ions and protons. The remaining acetic acid is then called the free acetic acid and is a potential source of corrosion (direct reduction at the metal surface). Moreover, both experiments are conducted with a liquid phase in the tank formed of a mixture water/glycol at 50%. It is not believed that glycol chemically reacts with acetic acid.

Top of the line

In SET 1, the concentration of free acetic acid in the tank is increased from 0 to 72 ppm when from SET 2, it is increased from 0 to 173 ppm. In both cases, the general corrosion rate does not seem to be affected, especially in the experiment 2-2 of SET 2 where the partial pressure of CO_2 is higher. The corrosion rate is also monitored using an ER probe in experiment 2-2 of SET 2. The result shows that both stable and average corrosion rate are in really good agreement with the corrosion rate obtained using weight loss coupons. In order to explain this result, several comments are made here. First, the concentrations of free acetic acid reported concern only the liquid phase of the tank. The concentration of free acetic acid in the condensed water at the top of the line is related to the one in the tank but is expected to be much lower. When the vapor condenses at the top of the line, it creates droplets or eventually a very thin film of liquid. As corrosion takes place, iron is released from the metal into the liquid which rapidly increases the pH. If the condensed liquid is not renewed rapidly enough (what is believed to be the case in these experiments), the pH keeps increasing and the acetic acid that condensates at the top consequently dissociates resulting in very little acetic acid remaining in the undissociated (free) form. Secondly, carbonic and acetic acids are the major two corrosive species (with water) and the level of corrosion is the result of their combined effect. Therefore, if the concentration of acetic acid is too low, its effect could be masked by the carbonic acid. This is especially true with high partial pressure of CO_2 (SET 2). Regarding a lower partial pressure of CO_2 of SET 1, a slight increase in the general corrosion rate is seen but it could be also due to variation in the results.

Bottom of the line

Regarding experiment 1-3 of SET 1, the general corrosion rate increases by one third at the bottom. Because some liquid is always flowing at the bottom, no increase in pH is expected and most of the acetic acid present remains in its undissociated form. The influence of 72 ppm of free acetic acid on the CO_2 corrosion is clearly seen here.
However, for experiment 2-2 of SET 2, the general corrosion rate at the bottom remains unchanged and unexpectedly low. The reasons for such a low corrosion rate are still unclear and are being further investigating.

Influence of the pH control

The effect of controlling the pH is studied in experiments and 1-3 to 1-6 of SET 1and in experiments 2-2 and 2-3 of SET 2 where sodium bicarbonate is introduced in the liquid phase of the tank

in order to reach the required value of pH. In all previous experiments, the pH reported is the pH measured in the tank and is dependant only on the partial pressure of CO_2 and acetic acid concentration.

Top of the line

Both experiments from SET 1 and 2 show little influence of pH control on the general corrosion rate at the top of the line. Regarding experiments from SET 1, it is important to notice that two values of pH have been tested (5.5 and 6.5) with different concentration of total acetic acid from 100 to 1000 ppm (See Table 4 for a complete description). In the same way, for experiments of SET 2, the pH in the tank is increased from its natural value ($\approx$ pH 4) to pH 6.8 and the concentration of total acetic acid is increased from 180 to 4000 ppm. The pH value has a strong influence on the chemistry of the liquid phase in the tank: high pH turns most of the acetic acid into acetate ions which do not evaporate, leaving a small amount of free acetic acid (around 40 ppm) available for the liquid/vapor equilibrium. Therefore, pH control will limit the amount of acetic acid in the vapor phase and consequently in the condensed water. A change of pH in the liquid phase in the tank will have no effect on the CO_2 partial pressure or on the condensation rate. For the top of the line corrosion, a pH-controlled environment is close to an acetic acid-free environment.

Bottom of the line

pH stabilization has a much stronger effect on the corrosion rate at the bottom of the line. That was not expected in our case since the liquid at the bottom of the line is supposedly predominantly formed from the condensed water (not subject to pH stabilization). It is believed that some liquid from the tank is carried over in the loop and influences the chemistry of the water at the bottom of the line. For experiments of SET 1, holding the pH at 5.5 (Test 1-4) lowered the corrosion rates considerably, while pH 6.5 lowered them even further. This is in agreement with the expected formation of protective layers of iron carbonate. The concentration of free acetic acid remains very low and does not influence the corrosion process as explained in the previous chapter. For experiment 2-3 of SET 2, the corrosion rate remains unexpectedly low and it is not clear if it is due to the pH stabilization or some other factors.

SURFACE ANALYSIS

Front view and cross section of top samples have been studied with or without corrosion product layer. The layer is removed according to the ASTM G1 standard. The main findings of this study are presented in this section.

Top of the line

Under all conditions tested for SET 1 and 2, iron carbonate crystals are always present on the surface of the samples from the top of the line (see Figure 10). However, the coverage of the surface is generally not uniform with areas with high density of crystals surrounded by regions where no crystals or crystals of smaller dimensions were found. First, this observation gives indications about the type of condensation process occurring at the top of the line: the vapor condenses in the form of droplets of liquid which remain attached at the surface of the coupon for a long enough time to create irregularities in the layer (see rounded areas on Figure 9). Secondly, it indicates that the iron concentration in the droplets of condensed water is such that there are conditions for iron carbonate precipitation. Inspection of samples after corrosion product removal also revealed that the attacked metal has a higher roughness in the areas where iron carbonate crystals were found, whereas the surrounding area seems to be smoother, suggesting differences in the corrosion kinetics (see Figure 11f). Most of the samples from

various experiments look similar and it is difficult to determine clearly the influence of each parameter on the corrosion process. The microscopic evidence suggests that the presence of acetic acid, glycol, and/or pH control under the experimental conditions studied had little effect on the general morphology and on the characteristics of the surface of the samples (with or without layer) from the top of the line.

Cross section analyses have been done for most of the top samples (see Figure 12). It is important to mention that in the SEM pictures shown, the magnification is always more than 200X. It is difficult to separate the specific influences of each of the parameters tested since, in all experiments conducted, the surface of the coupons appears to be similar. The metal profile of the corroded surface is usually very rough with a sharp morphology. Iron carbonate crystals are usually observed, and the layer adheres to the metal surface but quite porous. Although in some areas the attack seem to proceed faster than what is reflected by the general irregularities of the metal surface, it is believed that these observations are not enough to establish with certainty the initiation of localized corrosion. The roughness of the surface could be due to the natural uniform corrosion process. In order to be sure that localized corrosion is occurring, pits should be observed clearly at 40-100X. However, it is believed that test duration is a key factor in the observation of localized corrosion and the tests reported in this paper lasted only two to three days. Therefore, even if no clear evidence of localized corrosion is found, longer tests need to be done in order to confirm the presence or absence of localized corrosion and the influence of the different parameters on it.

CONCLUSIONS

- At the operational conditions of the two sets of experiments (low P_{CO2}, T = 80ºC, high condensation rate and high P_{CO2}, T = 70ºC, critical condensation rate) a non-protective, iron carbonate layer forms at the surface of the steel at the top of the line.

- At all the experimental conditions evaluated, the presence of glycol or acetic acid and the use of pH control had little visible effect on the general corrosion rate at the top of the line.

- Under the experimental conditions tested, it is not possible to establish with certainty the presence or the absence of localized attack at the top of the line. Due to the relatively short term of the experiments (2 to 3 days), it is difficult to differentiate between roughening caused by general corrosion and localized attack. It is believed that the experiment duration is too short to show any localized corrosion. Therefore, long term experiments need to be run in the future.

ACKNOWLEDGEMENTS

REFERENCES

1. Gunaltun Y.M., Supriyataman D., Jumakludin A., "Top of the line corrosion in multiphase gas line. A case history", Corrosion/99, paper No.36. (Houston, TX: NACE International, 1999)

2. Olsen S., Dugstad A., "Corrosion under dewing conditions", Corrosion/93, paper No.69. (Houston, TX: NACE International, 1993)

3. Gunaltun Y., Larrey D., "Correlation of cases of top of the line corrosion with calculated water condensation rates", Corrosion/00, paper No71. (Houston, TX: NACE International, 2000)

4. Pots B.F.M., Hendriksen E.L.J.A., "CO_2 corrosion under scaling conditions – The special case of top-of-the-line corrosion in wet gas pipelines", Corrosion/00, paper No.31. (Houston, TX: NACE International, 2000)

5. Van Hunnik E.W.J., Pots B.F.M., Hendriksen E.L.J.A., "The formation of protective $FeCO_3$ corrosion product layers in CO_2 corrosion", Corrosion/96, paper No.6. (Houston, TX: NACE International, 1996)

6. Vitse F., Khairul A., Gunaltun Y., Larrey de Torreben D., Duchet-Suchaux P., "Semi-empirical model for prediction of the top-of-the-line corrosion risk", Corrosion/02, paper No.2245. (Houston, TX: NACE International, 2002)

7. Vitse F., Gunaltun Y., Larrey de Torreben D., Duchet-Suchaux P., "Mechanistic model for the prediction of top-of-the-line corrosion risk", Corrosion/03, paper No.3633. (Houston, TX: NACE International, 2003)

8. Vitse F., "Experimental and theoretical study of the phenomena of corrosion by carbon dioxide under dewing conditions at the top of a horizontal pipeline in presence of a non-condensable gas", PhD thesis, Ohio University, 2002.

9. Sun Y., George K., Nesic S., "The effect of Cl^- and acetic acid on localized CO_2 Corrosion in wet gas flow", Corrosion/03, paper No.3327. (Houston, TX: NACE International, 2003)

10. Hedges B., McVeigh L, "The role of acetate in CO_2 corrosion: The double whammy", Corrosion 99, paper No.21. (Houston, TX: NACE International, 1999)

11. Crolet J.L., Thevenot N., "Role of free acetic acid on the CO_2 corrosion of steels", Corrosion 99, paper No.24. (Houston, TX: NACE International, 1999)

12. Singer M., Nesic S., Gunaltun Y., "Top of the line corrosion in presence of acetic acid and carbon dioxide", Corrosion 04, paper 4377. (Houston, TX: NACE International, 2004)

13. Gulbrandsen E., Morard J.H., "Why does glycol inhibit CO_2 corrosion?", Corrosion 98, paper No. 221. (Houston, TX: NACE International, 1998)

14. Oyevaar M., Morssinkof R., Westerterp R., "Density, viscosity, solubility, and diffusivity of CO_2 and N_2O in solutions of diethanolamine in aqueous ethylene glycol at 298 K", J. Chem. Eng. Data 34, 77-82, 1989.

15. De Waard C., Lotz U., "Prediction of CO_2 corrosion of carbon steel", Corrosion 93, paper No. 69. (Houston, TX: NACE International, 1993)

16. Halvrsen A.M.K., Anderson T.R, "pH stabilization for internal corrosion protection of pipeline carrying wet gas with CO_2 and acetic acid", Corrosion 03, paper No. 3329. (Houston, TX: NACE International, 2003)

17. Dugstad A., Dronen P.E, "Efficient corrosion control of gas condensate pipelines by pH-stabilization", Corrosion 99, paper No.20. (Houston, TX: NACE International, 1999)

18. Craig, Bruce, "Practical Oilfield Metallurgy and Corrosion", 2nd Edition, Metcorr (Denver, Colorado) p.14.

19. Gunaltun Y.M., Larrey D., "Correlation of cases of Top of the Line Corrosion with calculated water condensation rates", Corrosion 00, paper No.71. (Houston, TX: NACE International, 2000)

20. Joosten M.W. ,Kolts J., Hembree J.H., Achour M., "Organic acid corrosion in oil and gas production", Corrosion 02, Paper No. 02294. (Houston, TX: NACE International, 2002)

TABLES

Table 1. Brine Composition for SET 1

Ion	Concentration (mg/L)
Na^+	1,360.00
K^+	1.60
Mg^{2+}	0.80
Ca^{2+}	148.00
Fe^{2+}	5.00
Cl^-	3,300.00
SO_4^{2-}	5.10

Table 2. Chemical analysis of the carbon steels used in the experiments

Element	1020 Composition (%)	X65 Composition (%)	API 5L X65 Standard (%)	AISI 1020 Standard (%)
C	0.19	0.13	< 0.26	0.13-0.23
Mn	0.8	1.16	<1.40	0.30-0.60
P	0.01	0.009	< 0.03	< 0.04
S	0.023	0.009	< 0.03	< 0.05

Table 3. Hardness (HRB) results

	1020	X65 longitudinal cut	X65 transversal cut
1	83.5	81.3	60.3
2	84.5	94.4	68.7
3	82.1	98.7	63.3
4	89.1	87.9	78.0
5	83.2	95.4	59.1
6	86.8	89.3	51.1
7	80.9	88.7	66.5
8	80.2	92.9	75.0
9	89.1	93.3	58.5
10	83.2	85.1	67.7
Average	**84.3**	**90.7**	**64.8**
Approx.Tensile Strength	79,000psi for 85HRB	90,000 psi for 90.7HRB	56,000 psi for 65.7HRB
Tensile requirements	58,000 psi (min)	77,000psi (min)	77,000psi (min)
Yield Strength	36,000 psi (min)	65,000psi (min)	65,000psi (min)

Table 4. Experimental Matrix and Conditions for SET 1

Low CO$_2$ partial pressure - Liquid phase made of brine - T$_{gas}$= 80ºC

Experiment #		**1-0**	**1-1**	**1-2**	**1-3**	**1-4**	**1-5**	**1-6**	**1-7**
Investigating:		*Baseline*	*Cond rate*	*Glycol*	*HAc*	*pH*	*HAc*	*pH*	*HAc*
Condensation rate		Critical	High	High	High	High	High	High	High
Total HAc concentration (ppm) **Tank**	*Calculated*	*0*	*0*	*0*	*100*	*100*	*500*	*500*	*1000*
	Measured	0	0	0	73.8	87.1	494	N/A	855
Free HAc concentration (ppm) - **Tank** *Calculated*		*0*	*0*	*0*	*72*	*20*	*41*	*14*	*28*
Total HAc concentration (ppm) **Test section -** Measured		0	0	0	67	9.3	62.5	N/A	53.4
MEG in Brine (%) – **Tank**		*0*	*0*	*50%*	*50%*	*50%*	*50%*	*50%*	*50%*
MEG in condensed water (%) – **Test section**		0	0	6%	N/A	N/A	5%	N/A	N/A
pH measured - **Tank**		4.75	4.78	5.38	4.47	5.45	5.9	6.4	6.4
pH measured - **Test section**		N/A	4.3	3.69	3.11	N/A	N/A	N/A	N/A
Iron concentration (ppm) - **Tank**		N/A	N/A	7.27	9.62	2.53	1.34	1.99	0.67
Iron concentration (ppm) - **Test section**		N/A	N/A	2.55	5.14	N/A	0.89	2	1.5

Grey cell indicates a parameter that changes compared to a previous experiment.

Table 5. Experimental Matrix and Conditions for SET 2

High CO$_2$ partial pressure - Liquid phase made of de-ionized water - T$_{gas}$= 70°C

Experiment #		2-0	2-1	2-2	2-3
Investigating:		*Baseline*	*Glycol*	*HAc*	*pH HAc*
Condensation rate (mL/m^2.s)		Critical	Critical	Critical	Critical
Total HAc concentration (ppm) **Tank**	*Calculated*	*0*	*0*	*200*	*4000*
	Measured (CP)	0	0	168	4430
Free HAc concentration (ppm) - **Tank** *Calculated*		*0*	*0*	*173*	*40*
Total HAc concentration (ppm) **Test section** Measured		0	0	N/A	N/A
Glycol in de-ionized water (%) - **Tank**		0	50%	50%	50%
pH measured - **Tank**		3.82	3.8	4.04	6.83
pH measured - **Test section**		N/A	N/A	N/A	6.11
Iron concentration (ppm) - **Tank**		7.4	3.9	5.6	0.65
Iron concentration (ppm) - **Test section**		3.4	2.1	4.3	0.74

Grey cell indicates a parameter that changes compared to a previous experiment

FIGURES

Continuous injection of corrosion inhibitors is impossible

Water, glycol and acid vapor

CO_2

Injection of corrosion inhibitors is possible
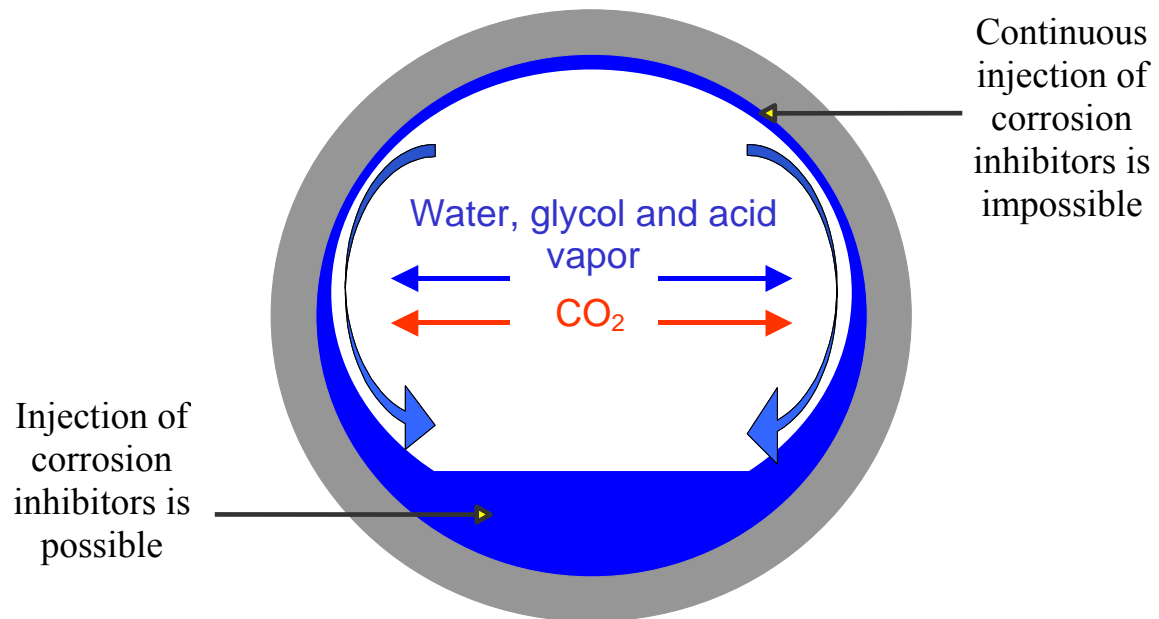
Figure 1. Schematic representation of the condensation inside the pipe

BACK

FRONT
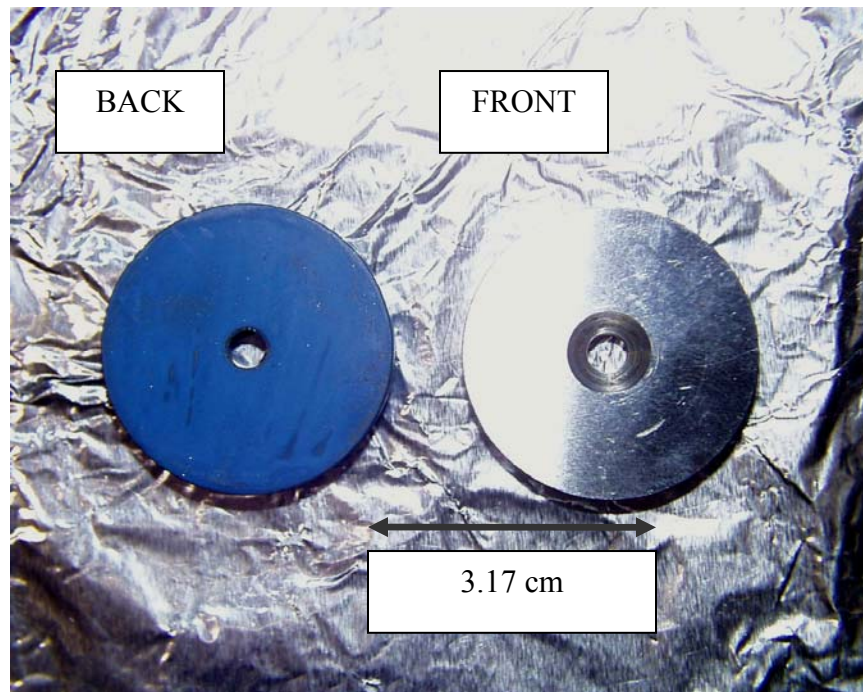
3.17 cm

Figure 2. Weight loss coupons with Teflon coating at the back and the side
(External diameter = 3.17 cm)
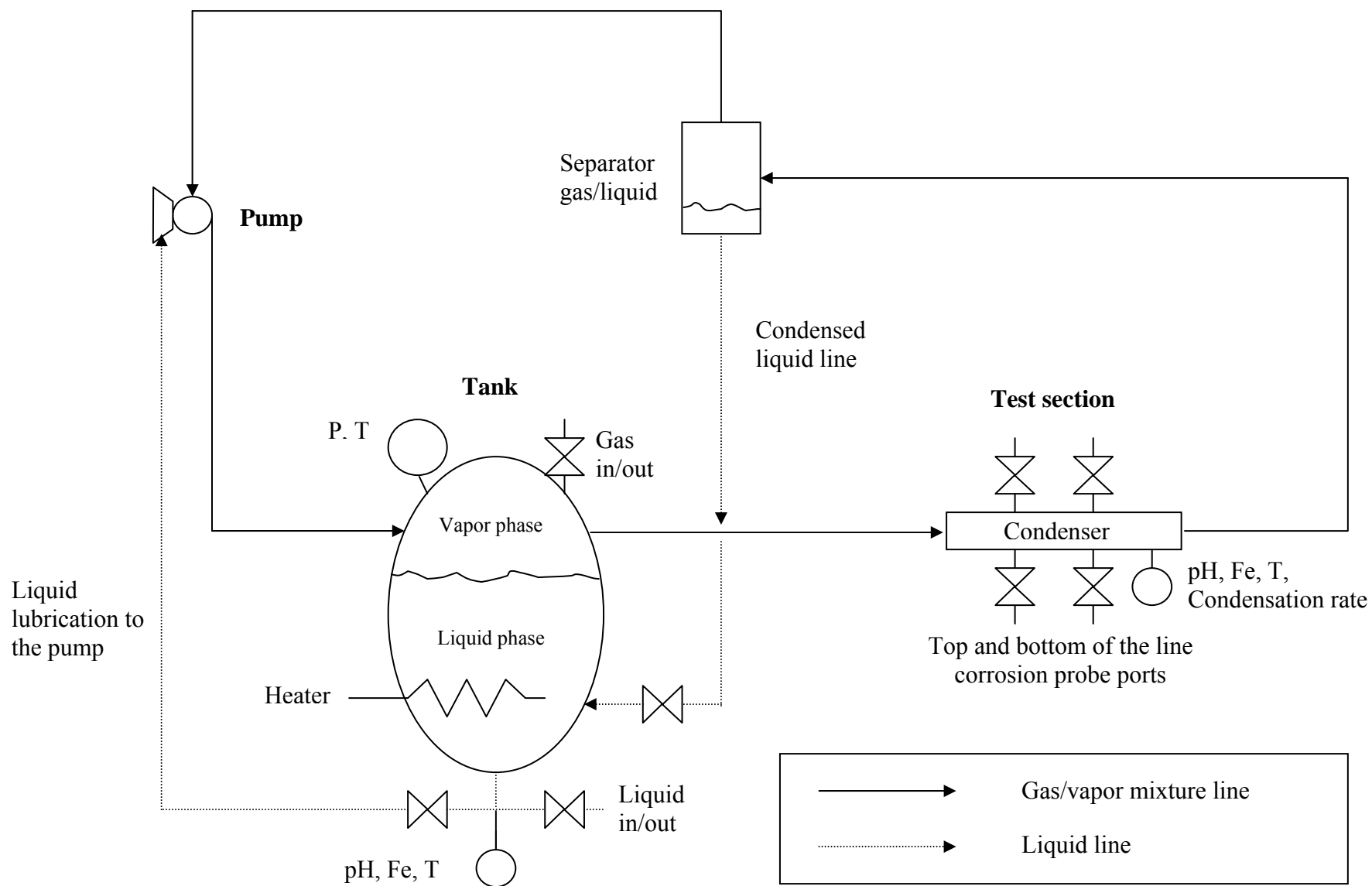
Figure 3. Loop schematic
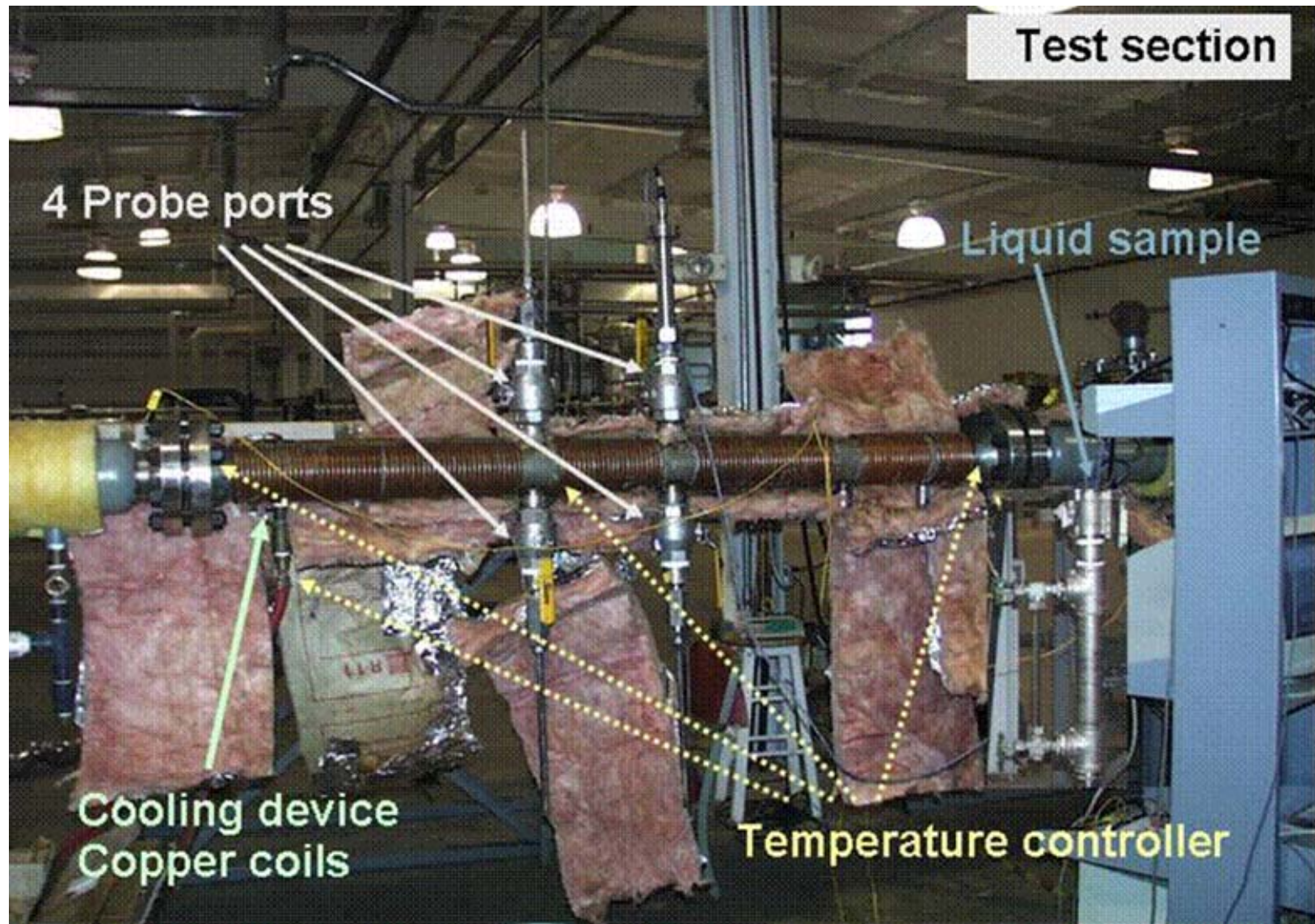
Figure 4. Picture of the test section
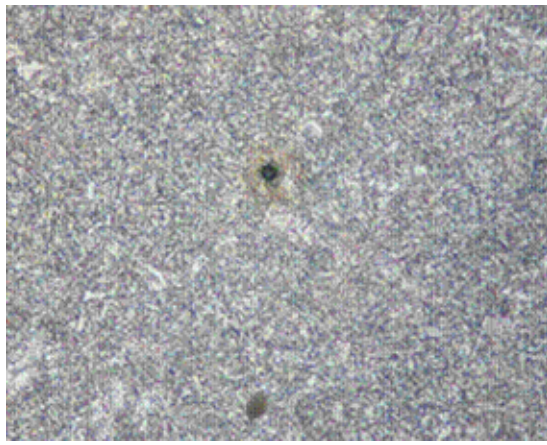
200X
(a)
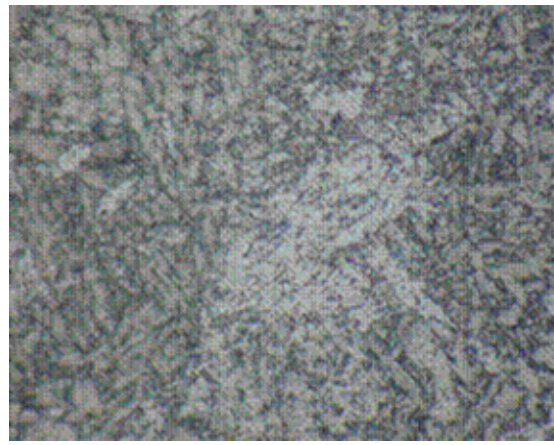
1000X
(b)

200X
(c)
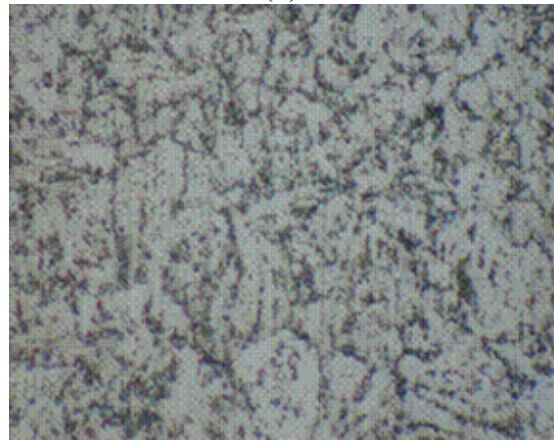
1000X
(d)

Figure 5. Microstructure of the X65 carbon steel
a-b) longitudinal cut, c-d) transversal cut
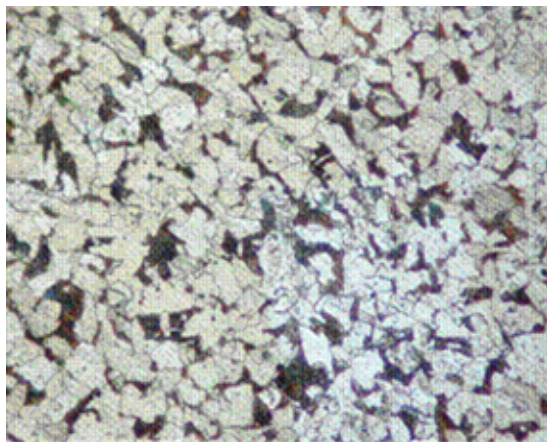
200X
(a)
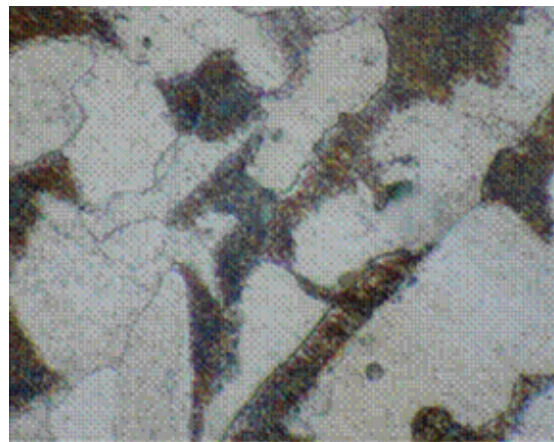
1000X
(b)

Figure 6. Microstructure of the 1020 carbon steel

Test Number	1-0	1-1	1-2	1-3	1-4	1-5	1-6	1-7
Free HAc ppm -Tank	0	0	0	72	20	41	14	28
pH (Tank)	4.75	4.78	5.38	4.47	5.45	5.90	6.40	6.40
MEG % (Tank)	0	0	50	50	50	50	50	50
Condensation rate	Critical	High	High	High	High	High	High	High
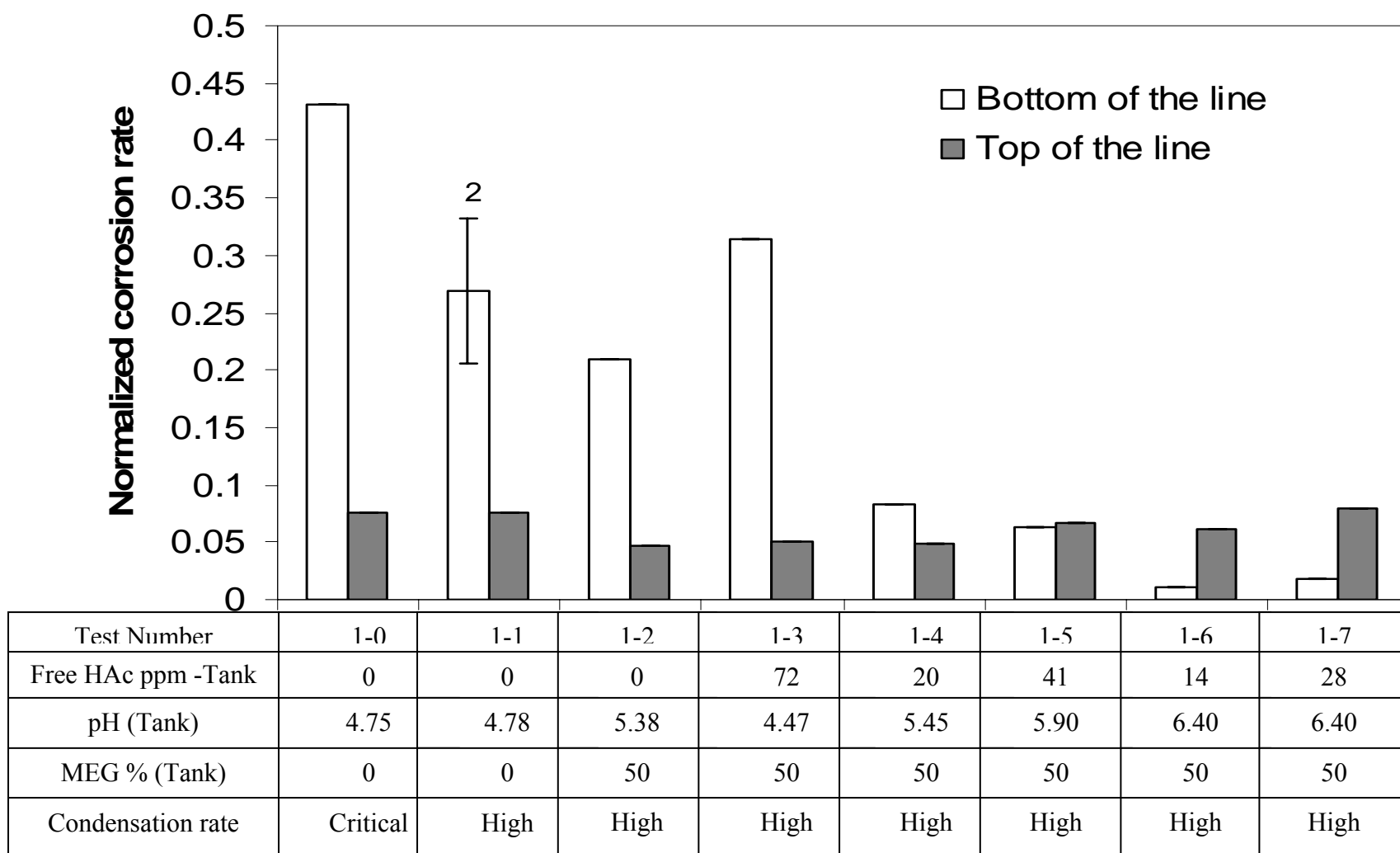
Figure 7. General corrosion rates for SET 1 experiments – Low pCO_2, T_{gas}=80C, Liquid phase: Brine

Test Number	2-0	2-1	2-2	2-3
Free HAc ppm -Tank	0	0	173	40
pH (Tank)	3.82	3.8	4.04	6.83
MEG % (Tank)	0	50	50	50
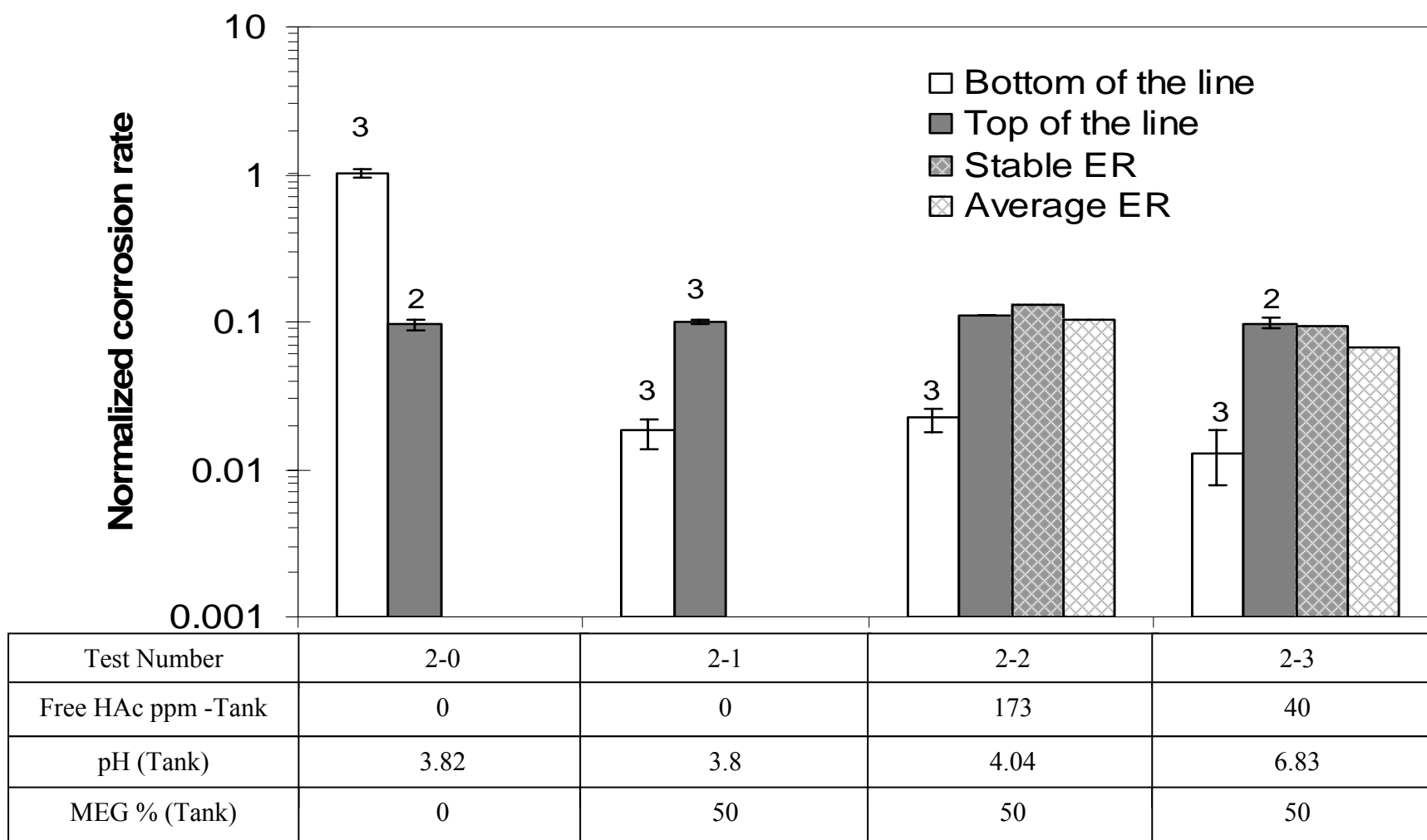
Figure 8. General corrosion rates for SET 2 experiments
High pCO_2, T_{gas}=80C, Liquid phase: de-ionized water, Critical condensation rate
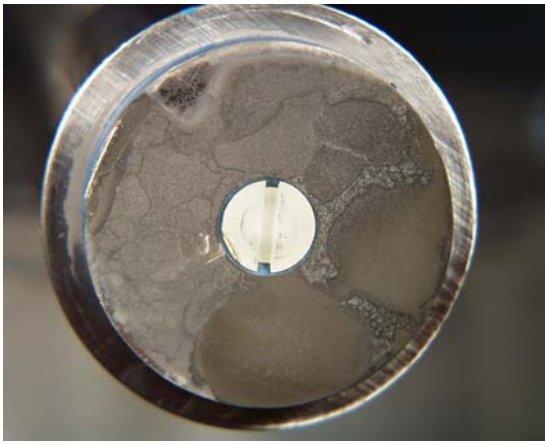
a) SET 1 / Test 1-2
Low pCO_2, 50% MEG, Free HAc= 0 ppm
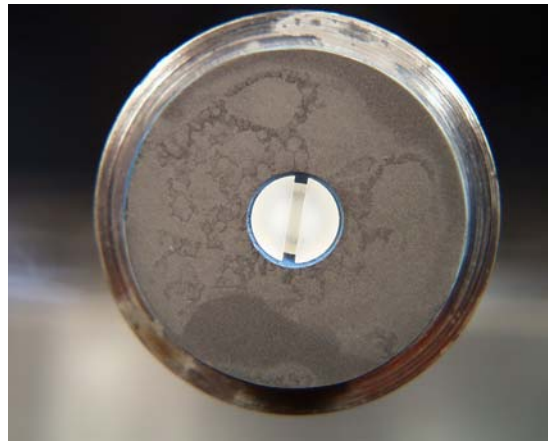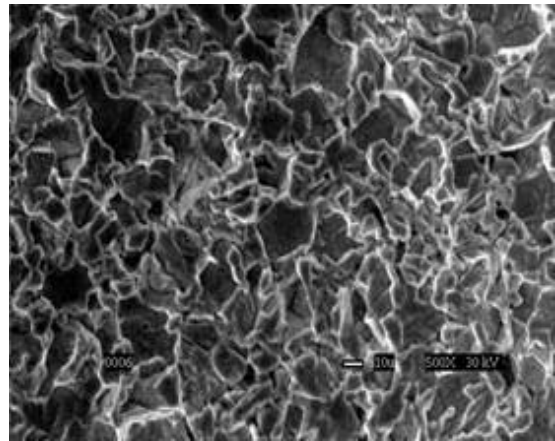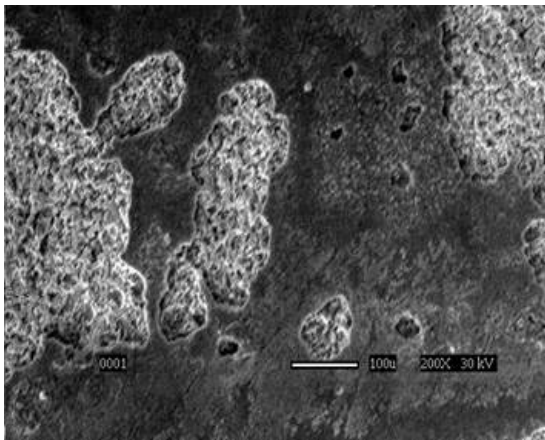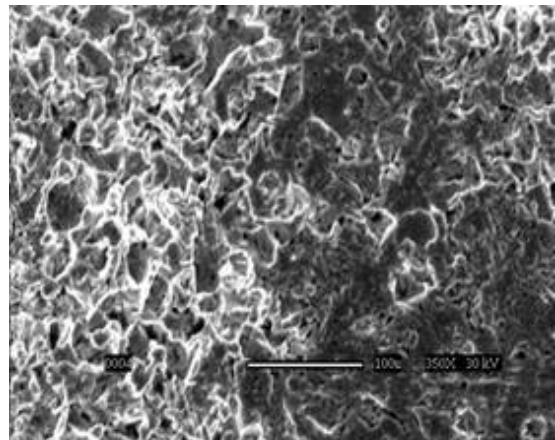
b) SET 2 / Test 2-1
High pCO_2, 50% MEG, Free HAc= 0 ppm
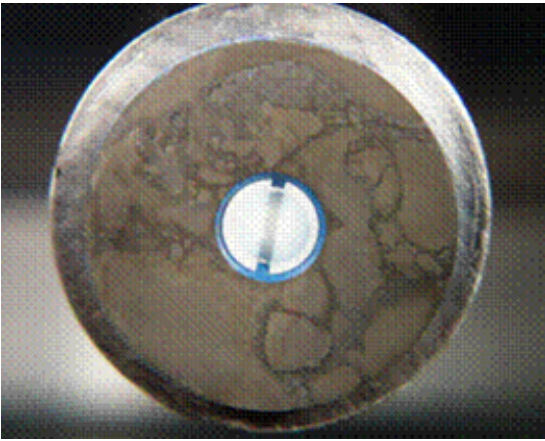
c) SET 1 / Test 1-4
Low pCO_2, 50% MEG, Free HAc= 20 ppm
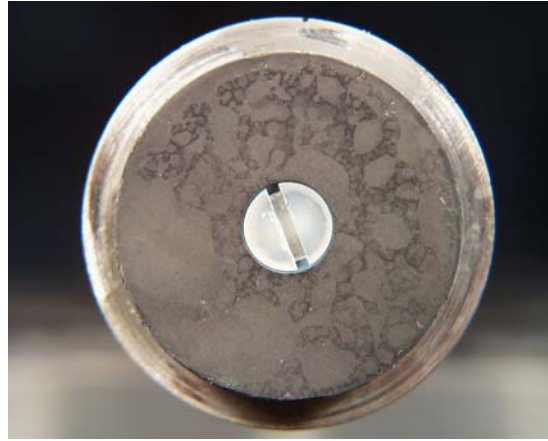
d) SET 2 / Test 2-3
High pCO_2, 50% MEG, Free HAc=40 ppm
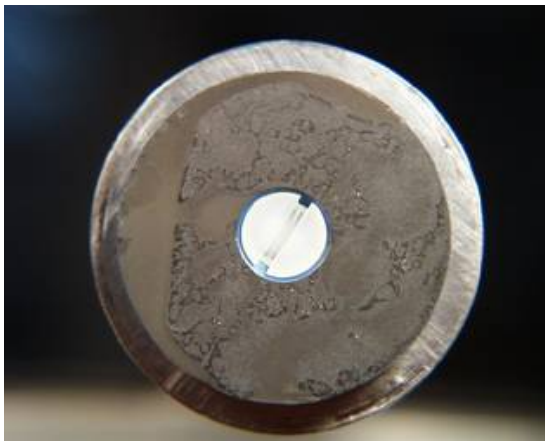
e) SET 1 / Test 1-7
Low pCO_2, 50% MEG, Free HAc= 28 ppm
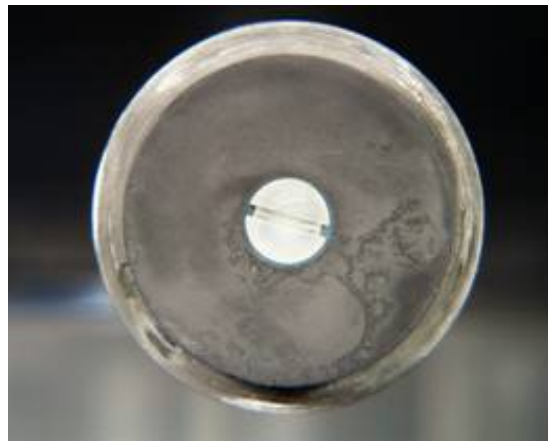
f) SET 2 / Test 2-2
High pCO_2, 50%MEG, FreeHAc=180 ppm

Figure 9. Pictures of top of the line coupons after test
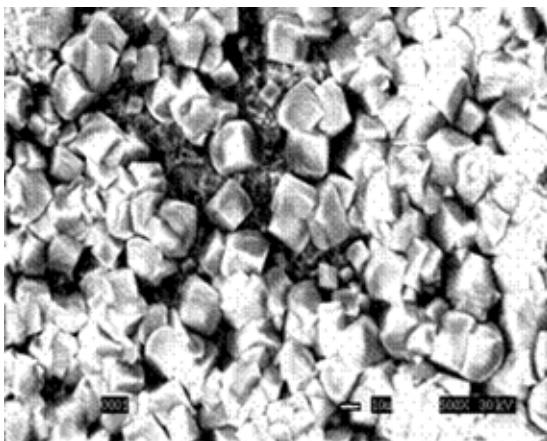
a) SET 1 / Test 1-0
Low pCO$_2$, 0% MEG, Free HAc= 0 ppm
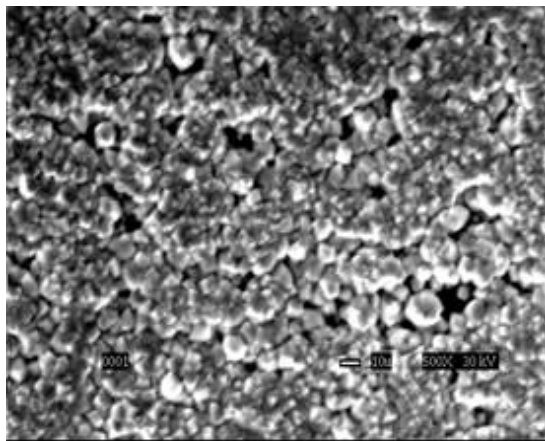
b) SET 2 / Test 2-0
High pCO$_2$, 0% MEG, Free HAc= 0 ppm
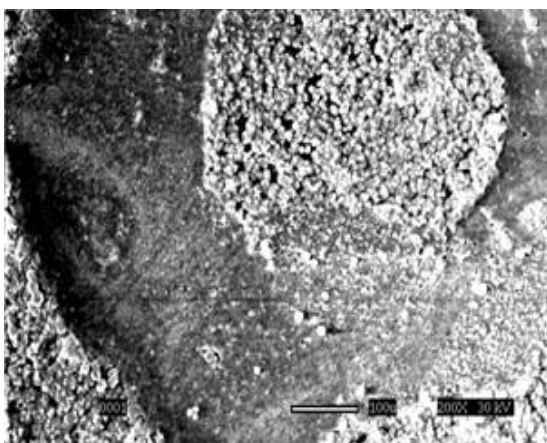
c) SET 1 / Test 1-7
Low pCO$_2$, 50% MEG, Free HAc= 28 ppm
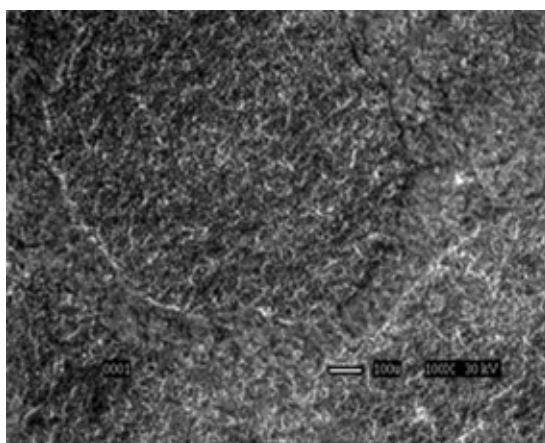
d) SET 2 / Test 2-3
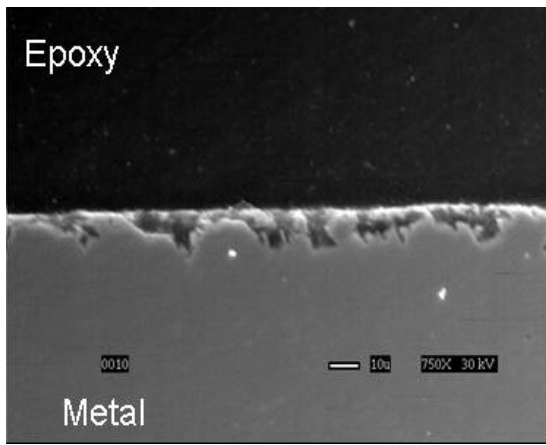High pCO$_2$, 50% MEG, Free HAc= 40 ppm
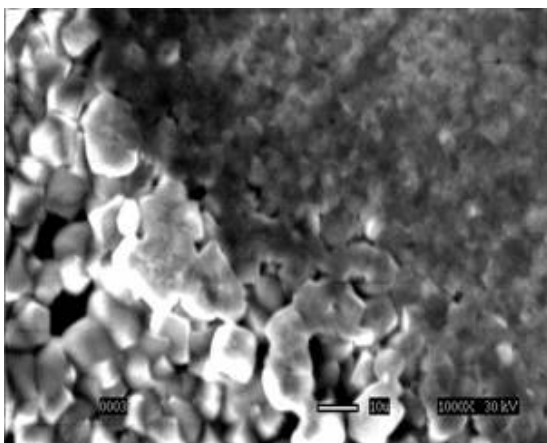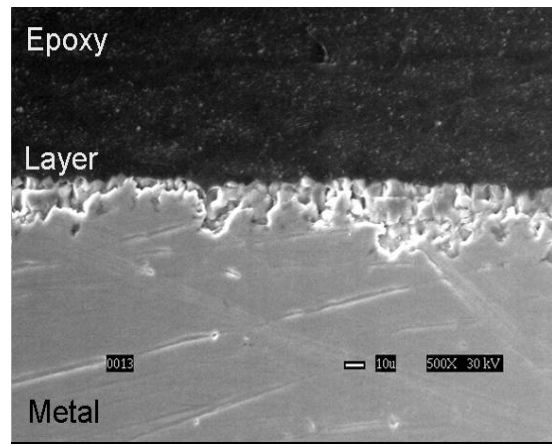
e) SET 1 / Test 1-7
Low pCO$_2$, 50% MEG, Free HAc= 28 ppm
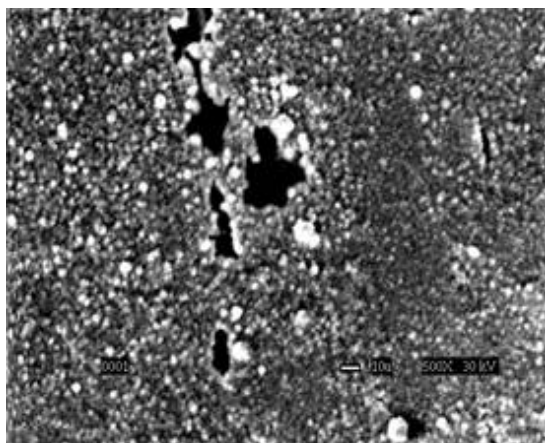
f) SET 2 / Test 2-2
High pCO$_2$, 50%MEG, Free HAc=180 ppm

Figure 10. SEM front views pictures of the iron carbonate layer – Top of the line samples
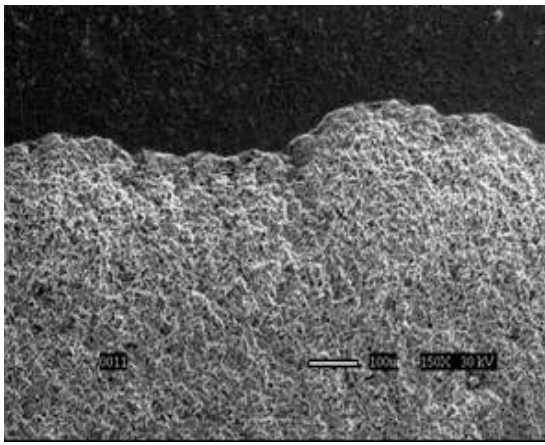
a) SET 1 / Test 1-0
Low pCO$_2$, 0% MEG, Free HAc= 0 ppm
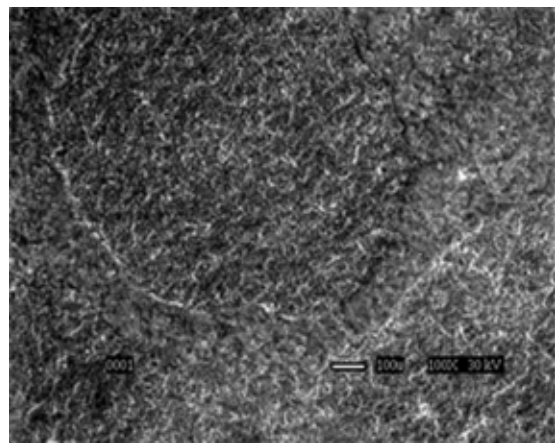
b) SET 2 / Test 2-1
High pCO$_2$, 50% MEG, Free HAc= 0 ppm
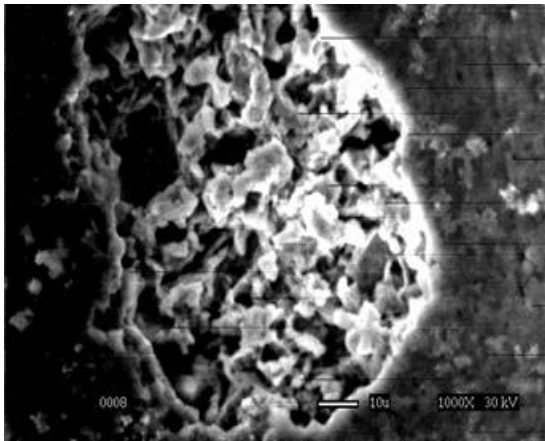
c) SET 1 / Test 1-3
Low pCO$_2$, 50% MEG, Free HAc= 72 ppm

d) SET 2 / Test 2-2
High pCO$_2$, 50%MEG, Free HAc=180 ppm

e) SET 1 / Test 1-5
Low pCO$_2$, 50% MEG, Free HAc= 41 ppm

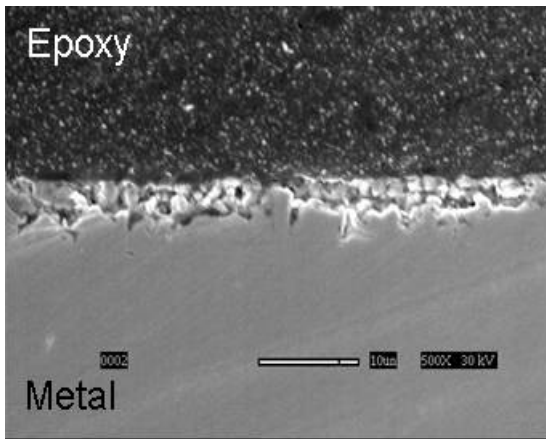f) SET 2 / Test 2-3
High pCO$_2$, 50% MEG, Free HAc= 40 ppm

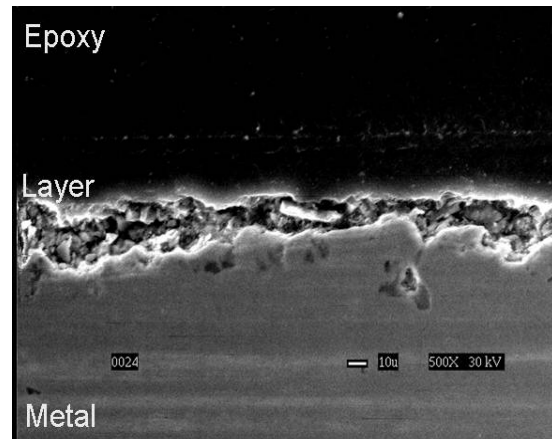Figure 11. SEM front views pictures of corroded surface after the removal of the layer Top of the line samples

a) SET 1 / Test 1-4
Low pCO$_2$, 0% MEG, HAc= 20 ppm

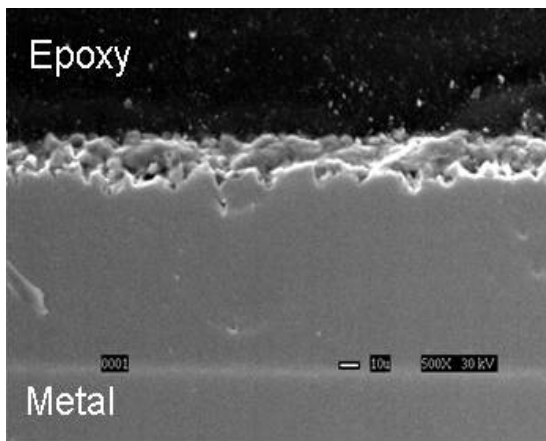b) SET 2 / Test 2-0
High pCO$_2$, 0% MEG, Free HAc= 0 ppm
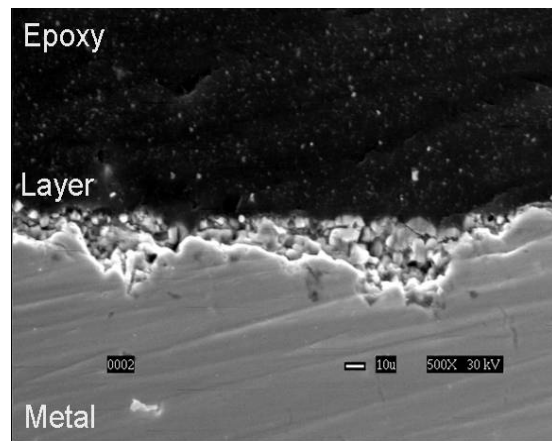
c) SET 1 / Test 1-5
Low pCO$_2$, 50% MEG, HAc= 41 ppm

d) SET 2 / Test 2-2
High pCO$_2$, 0% MEG, Free HAc= 180 ppm

e) SET 1 / Test 1-7
Low pCO$_2$, 50% MEG, HAc= 28 ppm

f) SET 2 / Test 2-3
High pCO$_2$, 50% MEG, Free HAc= 40 ppm

Figure 12. SEM cross section pictures of the coupons - Top of the line samples